

# Application of Supramolecular Nanostamping to the Replication of DNA Nanoarrays

Ozge Akbulut,<sup>†</sup> Jin-Mi Jung,<sup>‡</sup> Ryan D. Bennett,<sup>§</sup> Ying Hu,<sup>†</sup> Hee-Tae Jung,<sup>‡</sup> Robert E. Cohen,<sup>§</sup> Anne M. Mayes,<sup>†</sup> and Francesco Stellacci<sup>\*,†</sup>

*Department of Materials Science and Engineering, Department of Chemical Engineering, Massachusetts Institute of Technology, Cambridge, Massachusetts 02139, and Department of Chemical and Biological Engineering, Korea Advanced Institute of Technology, Daejeon 305-701, Republic of Korea*

Received August 17, 2007; Revised Manuscript Received September 27, 2007

## ABSTRACT

The rapid development of molecular biology is creating a pressing need for arrays of biomolecules that are able to detect smaller and smaller volumes of analytes. This goal can be achieved by shrinking the average size and spacing of the arrays' constituent features. While bioarrays with dot size and spacing on the nanometer scale have been successfully fabricated via scanning probe microscopy-based techniques, such fabrication methods are serial in nature and consequently slow and expensive. Additionally, the development of truly small arrays able to analyze scarce volumes of liquids is hindered by the present use of optical detection, which sets the minimum dot spacing on the order of roughly half the excitation wavelength. Here, we show that supramolecular nanostamping, a recently introduced truly parallel method for the stamping of DNA features, can efficiently reproduce DNA arrays with features as small as  $14 \pm 2$  nm spaced  $77 \pm 10$  nm. Moreover, we demonstrate that hybridization of these nanoarrays can be detected using atomic force microscopy in a simple and scaleable way that additionally does not require labeling of the DNA strands.

Arrays of biomolecules,<sup>1</sup> such as the ubiquitous DNA arrays,<sup>2</sup> with densely packed nanoscale features hold enormous promise for detection of analytes from small sample volumes and for analysis of large numbers of genes.<sup>1</sup> At present, there are only a few methods that allow the fabrication of DNA arrays with feature size and spacing below 100 nm. All of them are based on lithographic approaches to place or deliver DNA onto a specific location of a surface.<sup>3,4</sup> One of the most promising methods is dip pen nanolithography (DPN),<sup>3</sup> an approach in which a DNA "ink" placed onto the tip of an atomic force microscope (AFM) is released onto a surface. DPN has a feature resolution of 15 nm for simple molecules<sup>5</sup> and 50 nm for single strand DNA;<sup>3</sup> recently, with this method a two component DNA array was fabricated.<sup>3</sup> Other approaches, such as nanografting, also based on scanning probe lithography, have been used to make DNA arrays.<sup>4,6</sup> All of these methods are intrinsically serial, thus they can generate multicomponent arrays only if significant amounts of time are allocated. Even though some of these methods have been

parallelized recently by using multiple tip arrays,<sup>7,8</sup> scalability for multicomponent arrays remains a challenge.

Manufacturing time (and cost) is a major hurdle for nanoarrays, but it is not the only challenge. At present, most detection schemes are optical (the vast majority relying on fluorescence detection), hence they are limited by diffraction. For this reason, most fabricated nanoarrays have nanoscale features spaced micrometers apart.<sup>3</sup> At this spacing, it is questionable if there is any need for nanoscale features because the volume of the analyte scales with the overall array size and the advantages of small features are diminished by the disadvantages of large free surfaces prone to nonspecific adsorption and contamination. Hence, we reason that any manufacturing approach for nanoscale biological devices must be complemented with acceptable detection schemes that have resolution comparable to that of the fabrication scheme; examples in the literature include signal amplification schemes coupled with nanoparticle probes.<sup>9</sup>

Crooks' and our group have independently developed a method that is able to replicate DNA features from a master surface onto a secondary substrate in a truly parallel way.<sup>10,11</sup> This method is the only soft-lithography approach with the proven ability to stamp DNA features in a sequence-specific way. In principle, it could stamp a whole DNA array in a single cycle, that is, transfer the chemical and spatial

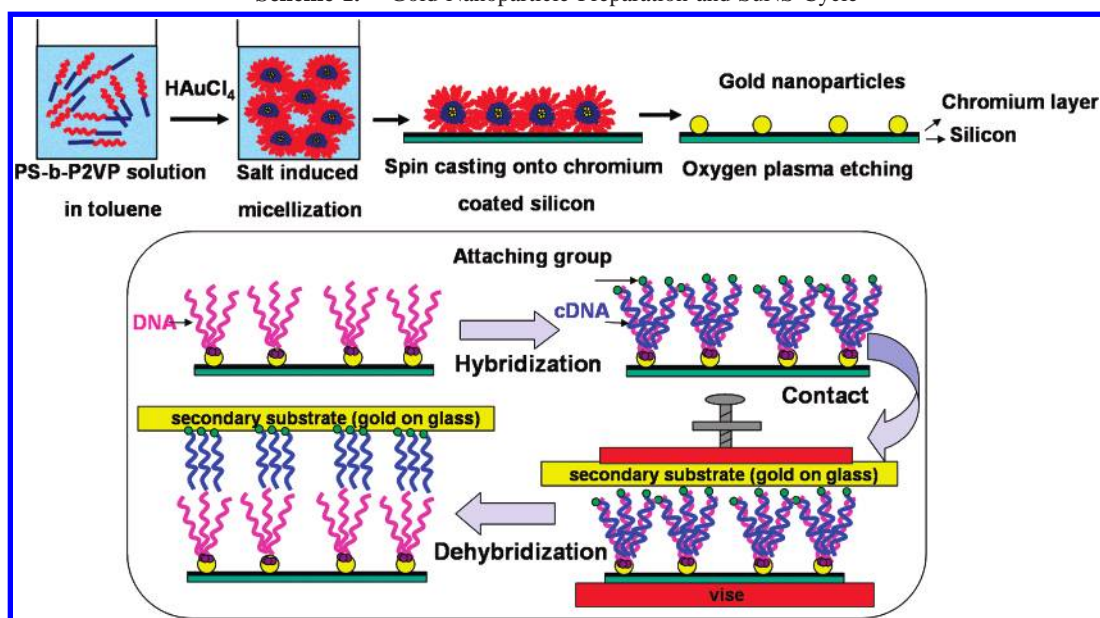
\* Corresponding author. E-mail: frstella@mit.edu.

<sup>†</sup> Department of Materials Science and Engineering, Massachusetts Institute of Technology.

<sup>‡</sup> Korea Advanced Institute of Technology.

<sup>§</sup> Department of Chemical Engineering, Massachusetts Institute of Technology.

Scheme 1. Gold Nanoparticle Preparation and SuNS Cycle



information of a master onto a secondary surface in a single step. Indeed, proofs-of-concept of such a single step stamping of DNA arrays have been published, employing two<sup>10</sup> and three<sup>12</sup> component arrays. We call our method supramolecular nanostamping (SuNS). It involves three steps: (1) hybridization, (2) contact, and (3) dehybridization, as shown in the boxed part of Scheme 1. A master made of single-stranded DNA features is immersed in a solution containing complementary DNA molecules terminated with chemical groups that can bind to a target surface (hybridization). Once hybridization has occurred, a secondary substrate is placed onto the master (contact) to allow for bond formation between this surface and the end groups of the complementary DNA strands. In our case, the master and the secondary substrate are then separated (dehybridization) by gentle heating whereas Crooks' approach is to separate mechanically.<sup>11</sup> Importantly, Crooks' group has also shown that cDNA strands can be enzymatically grown on the master with a "zip code" approach<sup>12</sup> thus making the extension to the stamping of whole microarrays an almost trivial exercise. Interestingly, SuNS has a significant resolution advantage over any other soft-material-stamping method<sup>13</sup> due to the absence of molecular diffusion during printing. Our group previously achieved a 50 nm resolution when printing on both hard and soft surfaces<sup>10,14</sup> thus demonstrating SuNS as an ideal candidate for the parallel and efficient mass production of nanoarrays. In the present study, we further probe SuNS' resolution limits by testing its ability to replicate features as small as 14 nm and hence made of only a few DNA molecules. Single-component master arrays were readily fabricated via a strategy based on the self-assembly of block copolymers (BCPs). This is, to the best of our knowledge, the best soft-material-stamping resolution<sup>3</sup> ever achieved and is also comparable to the best hard material results.<sup>15</sup> To complement this unprecedented feature resolution, we additionally propose an approach to hybridization

detection that has comparable resolution, based on the use of AFM as a hybridization detection tool on printed arrays.

To achieve arrays of DNA features on flat surfaces, thiolated DNA was attached onto an array of evenly spaced gold nanoparticles. There are many methods to obtain large area arrays of metal particles,<sup>16,17</sup> but only a few can produce arrays with sub-20 nm feature size and sub-100 nm particle spacing,<sup>18,19</sup> something needed in our application to facilitate imaging and hybridization. Here, we employed a published approach based on metal-loaded micelles of BCPs.<sup>18–21</sup> Briefly, an amphiphilic BCP, poly(styrene)-*block*-poly(2-vinylpyridine) (PS-*b*-P2VP), was dissolved in toluene, which is selective for poly(styrene), thus leading to the formation of core-shell structures. Metal precursor salt was selectively dissolved in the poly(2-vinylpyridine) core, and the solution was spin-coated onto a substrate to form a micelle monolayer. The organic components were subsequently removed via oxygen plasma treatment, leaving an ordered array of gold nanoparticles on the surface.<sup>18–21</sup> To have a master with sub-20 nm feature size and sub-100 nm spacing, an asymmetric BCP containing 780 styrene units and 200 2-vinyl pyridine units, PS<sub>780</sub>-*b*-P2VP<sub>200</sub>, ( $M_n(\text{PS}) = 81\,000\text{ g/mol}$ ,  $M_n(\text{P2VP}) = 21\,000\text{ g/mol}$ , PDI = 1.16) was used. The obtained gold features were  $9 \pm 2\text{ nm}$  in diameter and spaced  $77 \pm 9\text{ nm}$ , as evidenced by transmission electron microscopy (Supporting Information, Figure 1) and AFM images (Figure 1a). The ease and versatility of the process, that is, tunable spacing and partial control over feature size, as well as the capacity for large area coverage, makes these systems strong candidates for single-component nanoscale arrays.

According to Scheme 1, hexyl-thiol 5' modified single-stranded (50-mer) DNA (HS-ssDNA) was assembled on gold nanoparticles by a modification of the method described in Herne and Tarlov.<sup>22</sup> In brief, the gold nanoparticle-coated substrate was placed in a 5  $\mu\text{mol}$  HS-ssDNA buffered

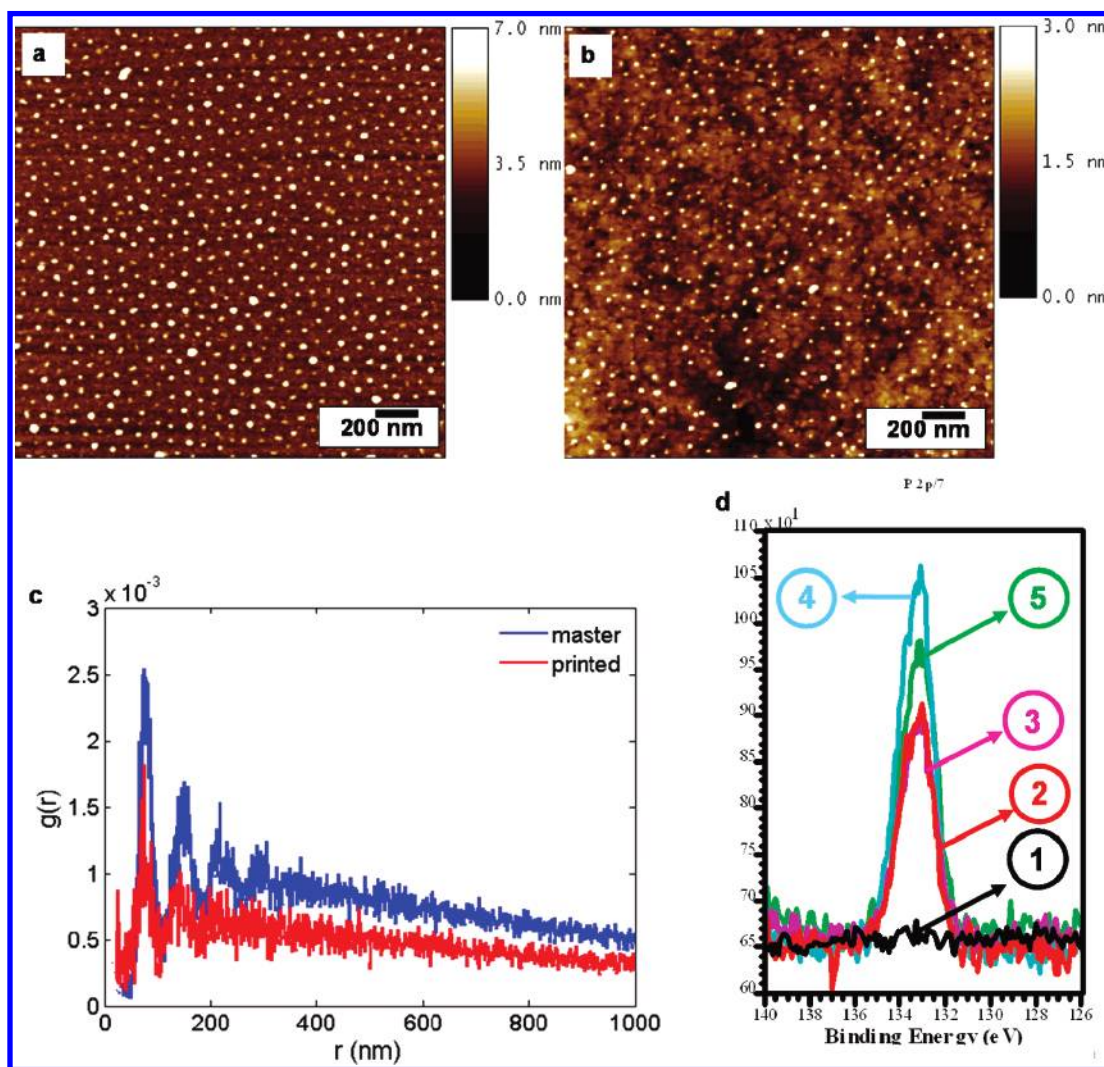


**Figure 1.** AFM height images of (a) gold nanoparticle master, (b) printed pattern, and (c) RDF comparison of (a) and (b). (d) XPS measurements (1) pristine gold nanoparticles (P/Au: 0), (2) ssDNA-immobilized gold nanoparticles (P/Au: 0.85), (3) MH treatment (P/Au: 0.77), (4) DNA-hybridized gold nanoparticles (P/Au: 1.47), and (5) master after printing/dehybridization (P/Au: 0.68).

solution. After thorough cleaning with deionized water, the substrate was immersed in a 1 mM 6-mercapto-1-hexanol (MH) aqueous solution to minimize nonspecific adsorption. AFM images of the substrate taken at various steps of this procedure showed no evident change in dot spacing. X-ray photoelectron spectroscopy (XPS) of the substrate over a  $5 \mu\text{m} \times 5 \mu\text{m}$  area performed before and after DNA assembly shows an increase of the average P/Au ratio from almost 0 to 0.85 thus proving the presence of DNA at least on the surface. Treatment with MH did not affect significantly this ratio (P/Au: 0.77). The DNA–gold nanoparticle array is referred to as the “master” hereafter. The master was then placed in a  $5 \mu\text{mol}$  solution containing DNA complementary to the one present on the master, 5' modified with hexylthiol (HS-cDNA), for 12 h to allow for hybridization. XPS revealed an approximate doubling of the P/Au ratio (from 0.77 to 1.47), confirming hybridization. The master was then brought into contact with a gold-on-glass substrate (see Supporting Information, Experimental Section for fabrication details on this substrate) using a vise, and light pressure was applied ( $<2$  atm as determined using Pressurex films by

Sensor Products LLC.). After 1 day in a desiccator, the vise was placed into an oven at  $90^\circ\text{C}$ . After 30 min, the vise was loosened, several drops of dehybridization buffer solution were placed onto the substrates, and the two were gently separated. XPS and AFM analyses made on the master show a return to the unhybridized state (P/Au: 0.68).

The printed substrate was investigated with AFM. Images showed the presence of nanometer-scale dots spaced by  $77 \pm 10$  nm (compared to  $77 \pm 9$  nm for the master) suggesting successful printing. (Occasional,  $<5\%$ , transfers of individual nanoparticles to the secondary substrate were also observed.) A typical printed pattern is shown in Figure 1b. To underscore the close match of the patterns, radial distribution functions were computed for both the master and the printed substrate patterns using image analysis software (ImageJ, National Institute of Health). As shown in Figure 1c, the radial distribution functions for both substrates are in close agreement, demonstrating that the feature arrangement observed on the printed substrate was derived from that present on the master. Upon decreasing the concentration of metal-loaded micellar BCP solution by a factor of 2, we



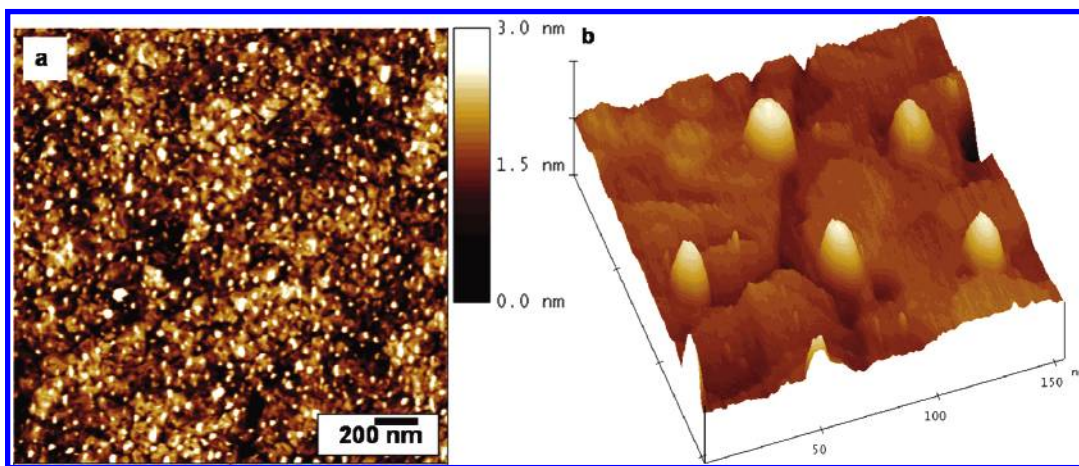


**Figure 2.** STM height image of the printed pattern (a)  $2\ \mu\text{m} \times 2\ \mu\text{m}$ , (b)  $150\ \text{nm} \times 150\ \text{nm}$ .

obtained a master with a particle spacing of  $90 \pm 10\ \text{nm}$  and a printed pattern spacing of  $86 \pm 10\ \text{nm}$  (data shown in Supporting Information, Figure 2).

AFM is a reliable and easy-to-use tool to detect printed DNA features and their spacing, but AFM images always show features whose shape is a convolution of the true feature shape and the tip shape itself. Hence, isolated features with sizes smaller than or comparable to the tip radius cannot be properly investigated using this technique. To truly determine the size of our printed array, scanning tunneling microscopy (STM) was performed on the printed DNA patterns. STM images of these arrays are more reliable, despite suffering from “combing” effects; that is, the alignment of the DNA molecules is roughly along the fast scanning direction of the tip. A good estimate of the feature size is then the size perpendicular to this direction. As shown in Figure 2, we printed  $14 \pm 2\ \text{nm}$  sized features. A rough calculation to estimate the number of printed DNA strands under the assumption of close packing would indicate the presence of at most  $\sim 50$  single strands in a  $14\ \text{nm}$  feature (see Supporting Information, Methods). However, the latter assumption does not agree with two experimental findings: close-packed DNA features should be as high as their extended length (as previously observed on other SuNS printed substrates)<sup>10</sup> and the shape of the DNA features should be almost insensitive to the scanning direction of an AFM or STM tip.<sup>10,23</sup> Our typical scanning probe microscopy data show a  $1\text{--}2\ \text{nm}$  height for printed DNA features compared to  $\sim 17\ \text{nm}$  for a fully extended 50-mer DNA,<sup>10</sup> indicating that DNA strands are lying flat on the surface rather than standing up in an extended confirmation. This picture is also consistent with the elongated shape observed in the STM images. Therefore, DNA strands appear to be far from close-packed, hence their number per feature must be less than 50.

As stated earlier, a significant challenge is to detect hybridization on such a dense array. To achieve this goal, we first passivated the free surface of the printed substrate with MH. It should be noted that AFM images of the substrate after passivation do not show an increase in height of the DNA features ( $1.09 \pm 0.33$  to  $0.99 \pm 0.24\ \text{nm}$ ). After MH treatment, the printed 50-mer DNA features were

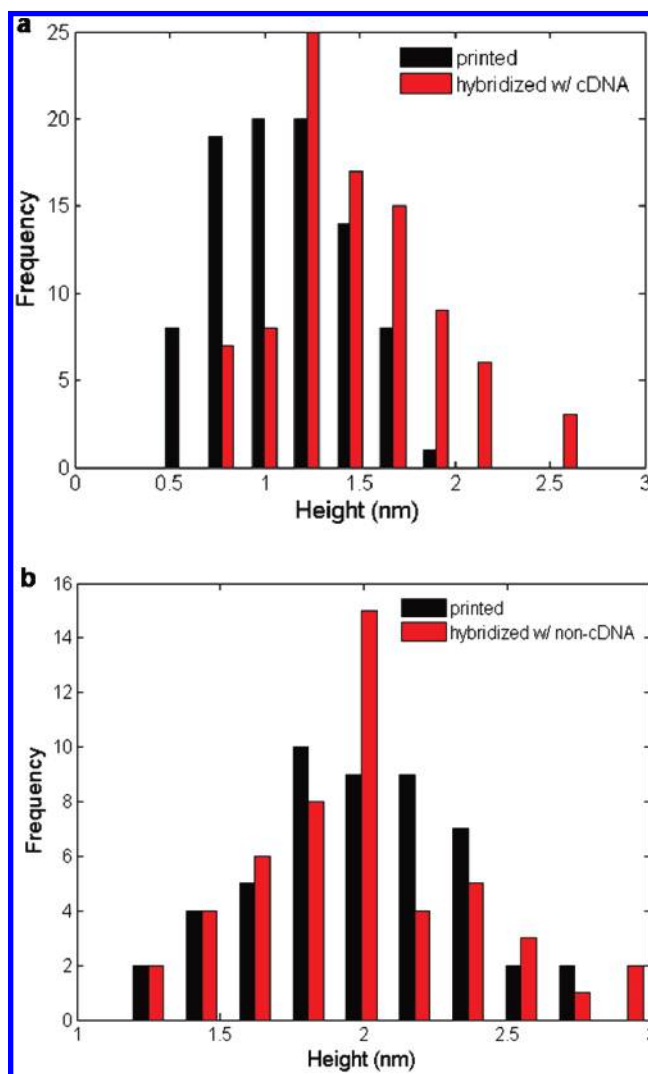


**Figure 3.** Height histogram of (a) printed pattern and hybridized pattern with complementary 50-mer DNA; (b) printed pattern and hybridized pattern with noncomplementary 50-mer DNA.

hybridized with 50-mer complementary DNA, and  $0.36\ \text{nm}$  height increase was observed ( $1.09 \pm 0.33$  to  $1.46 \pm 0.40\ \text{nm}$ ) (Figure 3a). A t-test analysis showed that the observed increase was statistically significant at the 0.01 level. When the substrate was exposed to a solution of noncomplementary

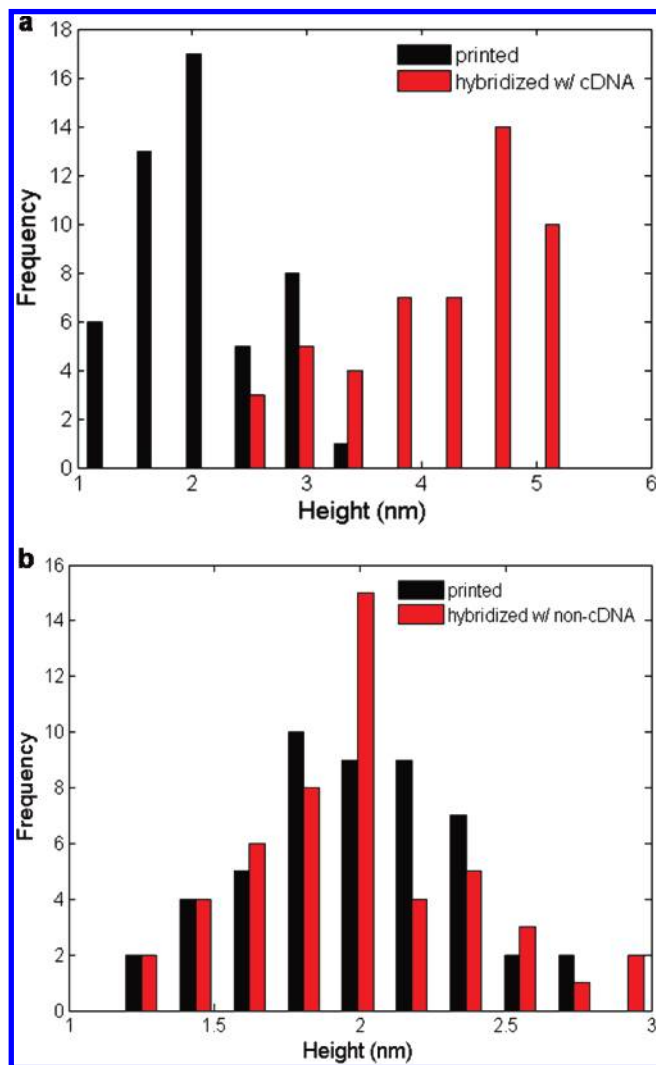


**Figure 4.** Height histograms of (a) printed pattern and hybridized pattern with complementary 100-mer DNA; (b) printed pattern and hybridized pattern with noncomplementary 100-mer DNA.

DNA strands (50-mer), the height increase was not statistically significant at 0.01 level (only statistically significant at the 0.7 level), the height averages were  $1.65 \pm 0.38$  and  $1.69 \pm 0.39$  nm for printed pattern and “hybridized” pattern respectively (Figure 3b).

To produce a more pronounced height increase (and incidentally a case closer to an array in use), the printed DNA array was exposed to a solution containing 100-mer DNA having the first half of its sequence complementary to that of the array. The average height of the printed DNA was  $2.08 \pm 0.57$  nm and the average height of the hybridized pattern was  $4.17 \pm 0.82$  nm. The comparative histogram is demonstrated in Figure 4a; a t-test reveals the heights are significantly different at the 0.01 level. By contrast, there was no statistical height increase when the hybridization was carried out with 100-mer noncomplementary DNA as shown in Figure 4b (the average heights were  $1.98 \pm 0.36$  and  $1.98 \pm 0.40$  nm for the printed pattern and hybridized pattern, respectively). AFM as a detection method has the additional advantage (besides nanoscale

resolution) of not requiring labeling of the DNA strands. We also speculate that height changes could be amplified (and consequently made easier to detect) by labeling the DNA with a bulky end group such as streptavidin.

It should be noted that, at present, the use of only one DNA sequence on the array and the variation in height of the printed features requires a statistical analysis for the determination of hybridization events. Assuming the use of at least 25 measurements, one would have to conclude that at the present dot spacing the resolution of the proposed detection approach is in the order of 400 nm. There is ample room for improvement. A better resolution would result if one of the following conditions could be achieved: (i) the distribution of heights of the printed pattern would not overlap with that of the hybridized patterns, (ii) multiple DNA arrays would be printed so to measure differential height between neighboring dots, and (iii) an alignment scheme would be in place so that height measurements could be performed on the exact same dots. We believe that single dot resolution is achievable.

In conclusion, we have demonstrated the applicability of SuNS for reproducing DNA nanoarrays by a simple master fabricated from metal-bearing BCP films. SuNS was used to replicate DNA features on 9 nm gold nanoparticles spaced by 77 nm with high fidelity. We also proposed and demonstrated AFM as a hybridization detection tool on nanometer scale DNA features via the detection of a height increase. Planned future work includes the demonstration of multicomponent arrays and multiple copies from a master and the determination of array sensitivity.

**Acknowledgment.** This work was supported by the MIT MRSEC Program of the National Science Foundation under Award DMR-0213282 and NSF-NER DMII-0303821. F.S. is grateful to the Packard Foundation for its generous award. The authors are grateful to Ayse Asatekin and Elizabeth Shaw for XPS measurements. O.A. and F.S. thank Dr. Arum Amy Yu and Sarah Thèvenet for valuable discussions.

**Supporting Information Available:** Experimental section. This material is available free of charge via the Internet at <http://pubs.acs.org>.

## References

- (1) Salaita, K.; Wang, Y.; Mirkin, C. A. *Nat. Nanotechnol.* **2007**, *2*, 145–155.
- (2) Moore, S. K. *IEEE Spectrum* **2001**, *38*, 54–60.
- (3) Demers, L. M.; Ginger, D. S.; Park, S.-J.; Li, Z.; Chung, S.-W.; Mirkin, C. A. *Science* **2002**, *296*, 1836–1838.
- (4) Zhou, D.; Sinniah, K.; Abell, C.; Rayment, T. *Angew. Chem., Int. Ed.* **2003**, *42*, 4934–4937.
- (5) Ginger, D. S.; Zhang, H.; Mirkin, C. A. *Angew. Chem., Int. Ed.* **2004**, *43*, 30–45.
- (6) Liu, M. Z.; Amro, N. A.; Chow, C. S.; Liu, G. Y. *Nano Lett.* **2002**, *2* (8), 863–867.
- (7) Minne, S. C.; Yaralioglu, G.; Manalis, S. R.; Adams, J. D.; Zesch, J.; Atalar, A.; Quate, C. F. *Appl. Phys. Lett.* **1998**, *(72)*, 3240–3242.
- (8) Wang, X. F.; Liu, C. *Nano Lett.* **2005**, *5*, (10), 1867–1872.
- (9) Taton, T. A.; Mirkin, C. A.; Letsinger, R. L. *Science* **2000**, *289*, 1757–1760.

- (10) Yu, A. A.; Savas, T. A.; Taylor, G. C.; Guiseppe-Elie, A.; Smith, H. I.; Stellacci, F. *Nano Lett.* **2005**, *5*, 1061–1064.
- (11) Lin, H.; Sun, L.; Crooks, R. M. *J. Am. Chem. Soc.* **2005**, *127*, 11210–11211.
- (12) Lin, H.; Kim, J.; Sun, L.; Crooks, R. M. *J. Am. Chem. Soc.* **2006**, *128*, 3268–3272.
- (13) Quist, A. P.; Pavlovic, E.; Oscarsson, S. *Anal. Bioanal. Chem.* **2005**, *381*, 591–600.
- (14) Yu, A. A.; Savas, T.; Cabrini, S.; diFabrizio, E.; Smith, H. I.; Stellacci, F. *J. Am. Chem. Soc.* **2005**, *127*, 16774–16775.
- (15) Gates, B. D.; Xu, Q.; Stewart, M.; Ryan, D.; Willson, C. G.; Whitesides, G. M. *Chem. Rev.* **2005**, *105*, 1171–1196.
- (16) Haynes, C. L.; Van Duyne, R. P. *J. Phys. Chem. B* **2001**, *105*, 5599–5611.
- (17) Kiely, C. J.; Fink, J.; Brust, M.; Bethell, D.; Schiffrin, D. J. *Nature* **1998**, *396*, 444–446.
- (18) Spatz, J. P.; Mössmer, S.; Hartmann, C.; Möller, M.; Herzog, T.; Krieger, M.; Boyen, H.-G.; Ziemann, P.; Kabius, B. *Langmuir* **2000**, *16*, 407–415.
- (19) Bennett, R. D.; Miller, A. C.; Kohen, N. T.; Hammond, P. T.; Irvine, D. J.; Cohen, R. E. *Macromolecules* **2005**, *38*, 10728–10735.
- (20) Glass, R.; Möller, M.; Spatz, J. P. *Nanotechnology* **2003**, *14*, 1153–1160.
- (21) Lu, J. Q.; Yu, S. *Langmuir* **2006**, *22*, 3951–3954.
- (22) Herne, T. M.; Tarlov, M. J. *J. Am. Chem. Soc.* **1997**, *119*, 8916–8920.
- (23) Zhang, R.-Y.; Pang, D.-W.; Zhang, Z.-L.; Yan, J.-W.; Yao, J.-L.; Tian, Z.-Q.; Mao, B. W.; Sun, S.-G. *J. Phys. Chem. B* **2002**, *106*, 11233–11239.

NL0720758